Acc. Chem. Res. **1999,** *32,* 854−861

Electron Transmission through Molecular Layers: Numerical Simulations and Theoretical Considerations

ABRAHAM NITZAN*

School of Chemistry, The Sackler Faculty of Exact Sciences, Tel Aviv University, Tel Aviv 69978, Israel

ILAN BENJAMIN

Department of Chemistry, University of California, Santa Cruz, California 95064

Received December 21, 1998

I. Introduction

Electron transfer, a fundamental chemical process underlying all redox reactions, has been under experimental and theoretical study for many years.[1] Theoretical studies of such processes seek to understand the ways in which their rate depends on donor and acceptor properties, on the solvent, and on the electronic coupling between the states involved. Such processes, which dominate electron transitions in molecular systems, are to be contrasted with quasi-free electron transport in metals and semiconductors. Electrochemical reactions, which involve both molecular and solid-state donor/acceptor systems, bridge the gap between these phenomena. Here, the electron transfer takes place between quasi-free electronic states on one side and bound molecular electronic states on the other.

The focus of the present discussion is another class of electron-transfer phenomena: electron transmission between two regions of free or quasi-free electrons through molecules and molecular layers. Examples for such processes are photoemission through molecular overlayers, the inverse process of low-energy electron transmission (LEET) into metals through adsorbed molecular layers, and electron transfer between metal and/or semiconductor contacts through molecular spacers.[2] A schematic view of the electronic states involved is shown in Figure 1: the manifolds {l} and {r} correspond to continua of free or quasi-free electron states in the substrates (or, depending on the process, in a vacuum), the middle box represents the molecule, and a set of levels {m} represents the molecular orbitals. The double arrows in the figure represent the couplings between the molecular states and the free electron states, and between the continuous manifolds.

Photoemission and LEET involve electrons of positive energy (relative to zero kinetic energy in a vacuum) and, as such, are related to normal scattering processes. Scanning tunneling microscopy (STM) and electron transmission in molecular bridges between conducting contacts involve negative energy electrons and, as such, are closely related to regular electron-transfer phenomena. In these cases, the traditional molecular view of electron transfer between donor and acceptor species gives rise to a novel view of the molecule as a current-carrying conductor. Observables such as electron-transfer rates and yields are replaced by conductivities or, more generally, by current−voltage relationships in such molecular junctions.

It should be obvious that, while the different processes outlined above correspond to different experimental setups, fundamentally they are controlled by similar physical factors. Broadly speaking, we may distinguish between processes for which *lifetimes* or *rates* (i.e., the time evolution) are the main observables and those which monitor *fluxes* or *currents*. In this Account, we focus on the second class, which may be further divided into processes that measure current−voltage relationships and those that monitor the nonequilibrium electron flux, e.g., in photoemission experiments.

A general expression for the conductivity of a one-dimensional junction in the linear response regime and at zero temperature is given by the Landauer formula,[3]

$$\sigma = \frac{e^2}{\pi\hbar} T(E_F) \tag{1}$$

where $T(E)$ is the transmission coefficient and E_F is the Fermi energy. The three-dimensional analogue of this result is given by the "multichannel Landauer formula",

$$\sigma = \frac{e^2}{\pi\hbar} N(E_F) \tag{2}$$

where $N(E)$ is the "cumulative reaction probability" at energy E.[4] In terms of the scattering matrix elements, $S_{if}(E)$, between an incident state i and a transmitted state f, both of energy E, this is

$$N(E) = \sum_i \sum_f |S_{if}(E)|^2 = Tr(SS^\dagger) \tag{3}$$

Abraham Nitzan was born in Israel in 1944. He received his B.Sc. in chemistry in 1964, his M.Sc. in physical chemistry in 1966 (with Prof. Gidon Szapski), both from the Hebrew University, and his Ph.D. in 1972 (with Prof. Joshua Jortner) from Tel Aviv University. He had a postdoctoral Fullbright Fellowship at MIT, was a research associate at the University of Chicago, and taught at Northwestern University before joining the Faculty at Tel Aviv University. At TAU he has been a Professor of Chemistry since 1982 and also served as Chairman of the School of Chemistry in 1984−7, and Dean of the Faculty of Science in 1995−8. Nitzan's reseach is in the field of chemical dynamics and transport phenomena in condensed phases. Recent work has focused on solvation and transport of ions in simple and complex solvents.

Ilan Benjamin was born in Israel in 1956. He received his B.Sc. in chemistry and physics from the Hebrew University of Jerusalem, where he also received his Ph.D. in theoretical chemistry in 1986, working under the direction of Professor Raphael Levine. He was a Weizmann Postdoctoral Fellow at the University of Pennsylvania, and he also held a postdoctoral appointment at UC San Diego. In 1989, he joined the faculty at UC Santa Cruz, where he is currently Professor of Chemistry. Benjamin's research interests include the theoretical and computational studies of relaxation processes and of chemical reaction dynamics in the condensed phase. In recent years, his research has focused on solvation, spectroscopy, and chemical reactions at liquid interfaces.

10.1021/ar970267b CCC: $18.00
Published on Web 09/03/1999

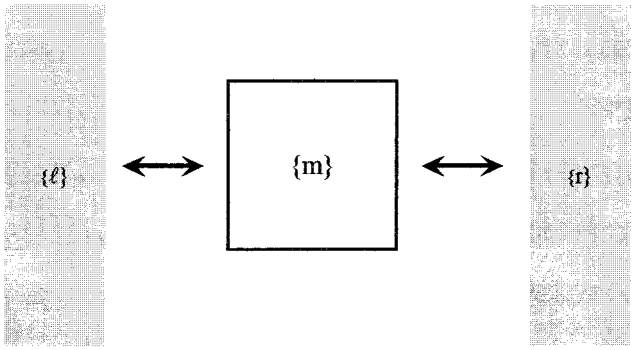

FIGURE 1. Schematic view of a model for electron transmission between two reservoirs through an intermediate manifold.

Here, the double sum corresponds to an "all-to-all" transition. In contrast, in a LEET experiment, the initial electron state may be sharply defined in terms of energy and direction, and the monitored signal corresponds to all possible final states. This signal is therefore proportional to

$$N_{i\to\{f\}}(E_i) = \sum_f |S_{if}(E_i)|^2 \tag{4}$$

In the photoemission experiment, the initial electron states span a broad energy range between zero and $\hbar\omega - W_F$, where ω is the exciting photon frequency and W_F is the substrate's work function. However, final state selection can be affected for the transmitted electron. If the optical excitation generates an electron distribution that is uniform in angular space, then the monitored signal is proportional to

$$N_{\{i\}\to f}(E_f) = \sum_i |S_{if}(E_f)|^2 \tag{5}$$

Thus, the two types of experiments convey equivalent information and are related to the transmission probability of the "one-to-all" type. In reality, however, the angular distribution of the photoelectrons is not necessarily isotropic, though this probably holds for the low-energy secondary electrons.

Calculating these quantities in realistic systems requires the evaluation of transmission probability through fairly complicated barriers. Some numerical approaches to this problem are discussed below.

2. Computation of Transmission Coefficients

Our objective is to compare electron transmission through a given molecular layer to the equivalent process in the absence of this layer, i.e., in a vacuum. In principle, two factors are involved: (a) the electrons, moving in the presence of the molecular spacer, suffer additional scattering by the molecules, and (b) the presence of the molecular layer on the substrate surface may change the electronic structure of the interface and, in turn, affect the interaction experienced by the electron. Here, we disregard the second factor and assume that the potential affecting the electron motion is a simple superposition of the vacuum potential and the electron−molecule coupling. The latter has been analyzed in two ways. The traditional quantum chemistry approach is to describe the molecular system in terms of its electronic structure: the molecular orbitals and their energies, populations, and interstate coupling. This is supplemented by the coupling between these orbitals and the states of the incident and scattered electron. This leads to the model displayed in Figure 1 and to expressions for the conductivity expressed in terms of the relevant molecular energy levels and the couplings between them.[5] This approach is useful for "negative energy" transmission phenomena because standard quantum chemistry methods needed to get the molecular orbitals {m} are not very reliable for energies above the molecular ionization.

An alternative approach to computing transmission is based on the pseudopotential method. Here, the detailed information about the electronic structure of the molecular spacer is replaced by the assumption that the electron scattering or tunneling can be described by a one-electron potential. Under our assumptions, the latter is a superposition of the potential experienced by the electron in the absence of the molecular spacer and the potential due to the electron−spacer interaction, written as a sum of interactions between the electron and the different atomic centers. The applicability of this method depends on our ability to construct reliable pseudopotentials of this type. In the work described below, we use the electron−water pseudopotential, derived and tested in studies of electron hydration,[6] and a modified pseudopotential that includes the many-body interaction associated with the water electronic polarizability.

Given such a potential, the problem is reduced to evaluating the transmission probability of an electron when it is incident on the molecular layer. Various time-dependent and time-independent numerical grid techniques were recently developed for such calculations. In the time-dependent mode, an electron wave packet is sent toward the molecular barrier and propagated on the grid using a numerical solver for the time-dependent Schrödinger equation. Since only the outcome at the end of the time evolution is needed, a propagation method based on the Chebychev polynomial expansion of the time evolution operator[7] is particularly useful.

In the time-independent mode, we apply the absorption boundary condition (ABC) Green's function technique following the formulation of Seidman and Miller.[8] Observables are obtained from sums over matrix elements of the Green's operator, $\hat{G}(E;\epsilon) = [E - \hat{H} + i\hat{\epsilon}(\mathbf{r})]^{-1}$. The absorbing potential $\epsilon(\mathbf{r})$ is taken to be different from zero near the grid boundaries in the transmission direction, far enough from the interaction region (i.e., the molecular barrier), and gradually decreasing to zero as the interaction region is approached from the outside. The grid representation of the Hamiltonian is a sparse matrix, suggesting the applicability of Krylov space-based iterative methods for this task.[9]

It should be emphasized that this outline of computational approaches assumes *static* barriers. The inherent assumption is that the electron transmission time is short

enough so that nuclear motions in the molecular barrier can be disregarded. Indeed, while nuclear dynamics is effective in electron transmission processes, as is observed, e.g., in inelastic tunneling spectroscopy, the contribution of the inelastic channel is often small. This can be rationalized by estimates of ∼1 fs for typical tunneling times in molecular junctions in the absence of resonance tunneling (see below). When the transmission is dominated by resonance levels in the molecular barrier, interaction times between electronic and nuclear motions can be considerably longer, and the static barrier approximation may break down. We do not have, at present, a reliable numerical approach to transmission under such conditions.

3. Transmission through Water[10−16]

Water constitutes a special medium for electron transmission because of its prominent role as the main environment for dielectric solution chemistry. Continuum dielectric theory has played a key role in developing our ideas on charge-transfer processes in such environments. Later systematic improvements, such as nonlocal dielectric response, nonlinear response, first-shell effects, classical molecular dynamic (MD) simulations, and quantum dynamical simulations, were discussed and compared for this solvent.

Electron transmission through water is obviously an important element in all electron-transfer processes involving hydrated solutes and in many processes that occur in water-based electrochemistry. In what follows, we focus on negative energy (tunneling) processes and on positive energy transmission processes at energies below the lowest excited electronic state of water (6.7 eV), so electronic excitation of the water molecules can be disregarded. In addition, photoemission through water layers adsorbed on metals,[17] as well as calculations of electron transmission[10] and electron tunneling[18] through water, indicates that inelastic processes associated with the water nuclear motion contribute relatively weakly at such energies. This can be rationalized by the short interaction time: for tunneling processes, taking typical values for a barrier height ∼1 eV, and for a barrier width of 5 Å, the tunneling time estimated from the Buttiker−Landauer theory[19] is ∼1 fs. Thus, the static medium assumption appears to provide a reasonable basis for discussing the overall transmission. It should be emphasized, however, that while solvent nuclear motion is slow relative to this time scale, solvent electronic response (electronic polarizability) is not. We return to this issue below.

The simulations described below, of electron transmission through static water layers, illustrate the principal factors affecting the transmission process. We consider (a) the dimensionality of the process, (b) the effect of layer structure and order, (c) the effect of resonances in the barrier, and (d) the signature of band motion. The simulations consist of, first, preparing water layer structures on (or between) the desired substrates using classical MD simulations; second, choosing appropriate electron−water and electron−substrate pseudopotentials; third, setting the Schrödinger equation for the electron transmission problem on a suitable grid; and, finally, computing the transmission probabilities using time-dependent or time-independent approaches. Two important points should be emphasized:

(a) For the water−water interaction used in the MD preparation stage, we have used both the RWKM-2 potential that was previously used in studies of electron solvation in water clusters[20] and also a polarizable flexible simple point charge model (PFSPC) which includes a sum over two-body Lennard-Jones plus Coulomb interactions between the atomic sites and a many-body contribution due to the polarizable nature of the oxygen and hydrogen atoms.[21] In general, we have found[12,13] that water layers prepared with these different interaction models had similar transmission properties.

(b) Most previous studies of electron solvation in water represent the electron−water pseudopotential as a sum of two-body interactions. In our studies of electron hydration and hydrated electron spectroscopy, we have found that the potential developed by Barnett et al.[6] could account semiquantitatively for the general features of electron solvation structure and energetics in bulk water and in water clusters. Taking into account the many-body aspects of the electronic polarizability contributions to the electron−water pseudopotential[22] has led to improved energy values that were typically different by 10−20% from the original results. In contrast, including these many-body interactions in the tunneling calculation is found (see below) to have a profound effect: an increase of ∼2 orders of magnitudes in the transmission probability of electron through water in the deep tunneling regime. There are two reasons for this. First, as already noted, tunneling processes are fast relative to characteristic nuclear relaxation times. The latter is disregarded, leaving the electronic polarizability as the only solvent response in the present treatment. Second, variations of the interaction potentials enter exponentially into the tunneling probability, making their effects far larger than the corresponding effect on solvation.

Including the solvent electronic polarizability in simulations of quantum mechanical processes in solution raises some conceptual difficulties. Our approach to this problem is described in refs 12 and 13. In what follows, we refer to the different models used in our studies as follows:

(1) For the electron−water interaction, model A uses the original pseudopotential of Barnett et al.,[6] while model B includes the many-body aspects of the water electronic polarizability as discussed above.

(2) For the water force field and for the water−substrate interaction, model 1 uses RWKM-2 water with an uncorrugated model gold surface with 9-3 interaction potential with the hydrogen and oxygen atoms of each water molecules.[23] Model 2 uses PFSPC water between two Pt (100) plates, with water−metal interaction determined as

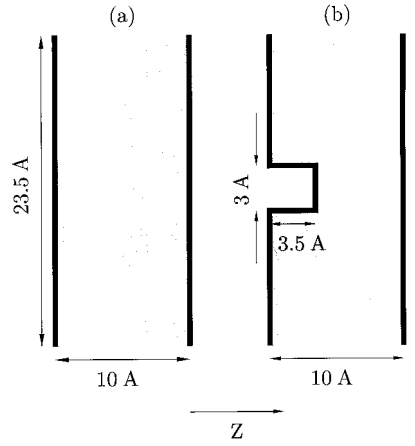

FIGURE 2. Schematic two-dimensional view of configurations used in model simulations of electron transmission through water: (a) Two parallel electrodes; (b) two parallel electrodes with an additional rectangular tip. Only model a is discussed in the present Account.

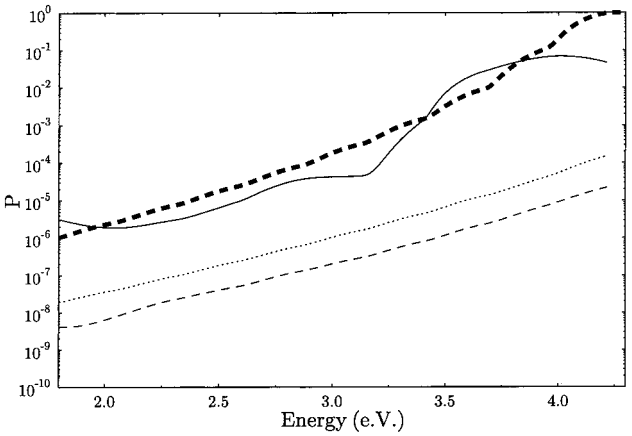

FIGURE 3. Electron tunneling probabilities through different model barriers. See text for details.

a sum of the O−Pt and H−Pt pair interactions taken from the work of Spohr and Heinzinger.[24]

In what follows, we refer by models A1, A2, B1, or B2 to the corresponding combinations of pseudopotential and water−substrate models. As already noted, the differences between models 1 and 2 for the water and substrate had relatively small effects on the computed transmission. The simulations results described below were obtained in the configuration shown on the left side of Figure 2. (Results of simulations done with the "tip" configuration displayed on the right are shown in ref 11.) Unless otherwise stated, the vacuum potential that is superimposed on the electron−water potential is represented here by a square barrier of height 5 eV, and the total transmission probability is calculated for an electron incident normal to the water layer.

Figure 3 shows results of such calculations for the transmission probability as a function of the incident electron energy, averaged over six equilibrium water configurations. These configurations are sampled from an equilibrium trajectory for what we will refer to as the *standard system*: 192 water molecules confined between two walls separated by 10 Å, with periodic boundary conditions with period 23.5 Å in the directions parallel to

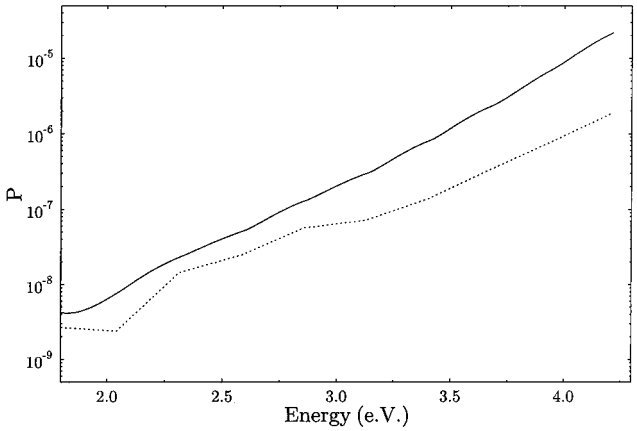

FIGURE 4. Electron tunneling probabilities through water between two electrodes with (full line) and without (dotted line) orientational ordering at the metal wall.

the walls, at 300 K. These data correspond to three water monolayers between the walls. Figure 3 shows results obtained using model A (thin-dashed line) and model B (full line). Also shown are the corresponding results for tunneling through a vacuum, i.e., through a bare rectangular potential barrier of height 5 eV (dotted line), and through a similar barrier of height 3.8 eV (thick-dashed line), which corresponds to the expected lowering of the effective barrier for tunneling through water. The results for the polarizable model are seen to be in remarkable agreement with the expectation based on lowering of the effective rectangular barrier by 1.2 eV.

Next we consider the effect of orientational ordering of water dipoles on the metal walls. Water adsorbs with its oxygen on the metal surface and the hydrogen atoms pointing away from it, leading to net surface dipole density directed away from the wall. Simulations yield $\sim 5 \times 10^{-11}$ Coulomb/m for this density.[25] This is an important factor in the reduction of the surface work function of many metals due to water adsorption.[26] Figure 4 compares, for model A1, the transmission probabilities computed with two water configurations ("standard" geometry): one obtained using interaction model 1 as before, and the other obtained from a similar model in which the attractive oxygen−metal wall interaction, and therefore the preferred orientational ordering, was eliminated.[11] We see that the existence of a surface dipole in the direction that reduces the work function is associated with a larger transmission probability, as expected.

Traditional approaches to electron transfer are based on a continuum dielectric picture of the solvent, where the issue of tunneling path rarely arises. Barring other considerations, the exponential dependence of tunneling probabilities on the path length suggests that the tunneling process will be dominated by the shortest possible, i.e., one-dimensional, route. A closer look reveals that electron tunneling through water is inherently three-dimensional (see, e.g., Figure 7 of ref 11). An interesting demonstration of the importance of the 3-D structure of the water layer in determining the outcome of the tunneling process is shown in Figure 5.[14] Here, we use water layers prepared at room temperature using model B1 in

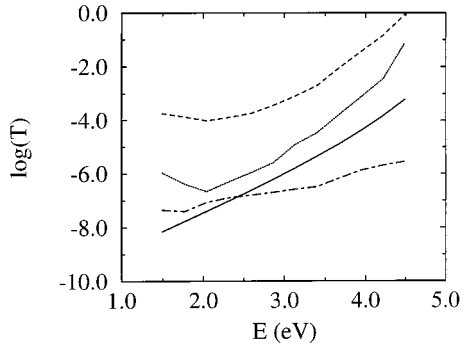

FIGURE 5. Electron transmission probabilities between the two walls described in the text. Full line, vacuum tunneling (bare barrier, 5 eV); dotted line, normal equilibrium water configuration (model B1); dashed and dashed−dotted lines, water oriented by a field 5 eV/Å with tunneling direction opposite and identical to the orienting field, respectively.

the "standard" geometry. Figure 5 shows the "one-to-all" transmission probability for an electron incident in the normal (z) direction on the 10 Å water layer lying in the xy plane. It compares vacuum tunneling to tunneling through a regular water layer and through another water configuration that was prepared in the presence of a strong electric field pointing along the tunneling (z) axis. In the resulting layer structure, the water dipoles point, on the average, along this axis. The electric field that was used to generate this order is removed during the tunneling calculation. In the statistically symmetric normal water layer, the tunneling probability does not depend on the tunneling direction, positive or negative, along the z-axis. Microscopic reversibility implies that the same should be true also in the oriented asymmetric layer in any one-dimensional model. In the three-dimensional calculation, we find several orders of magnitude difference between the one-to-all transmission probabilities calculated for electron incident on the layer in the direction of the induced polarization and against this direction. This shows that the angular distribution associated with the transmission through such a layer depends strongly on the transmission direction and suggests that asymmetry in the current−voltage dependence of transmission current should exist beyond the linear regime. Recent STM results in water by Pan, Jing, and Lindsay[27] and by Hong, Hahn, and Kang[28] show some evidence for this asymmetry.

Next, we consider the possibility of resonance-assisted tunneling. Figure 6[29] shows such resonances below the 5 eV vacuum barrier. The existence of such resonances correlates with the observation of weakly bound states of an electron in neutral configurations of bulk water. We have found[12] that such states appear in neutral water configurations in both models A and B; however, only model B shows such states at negative energies. Moreover, these states are considerably more extended in systems described by model B compared with the corresponding states of model A.[12] We emphasize again that, because these results were obtained for static water configurations, their actual role in electron transmission through water is yet to be clarified.

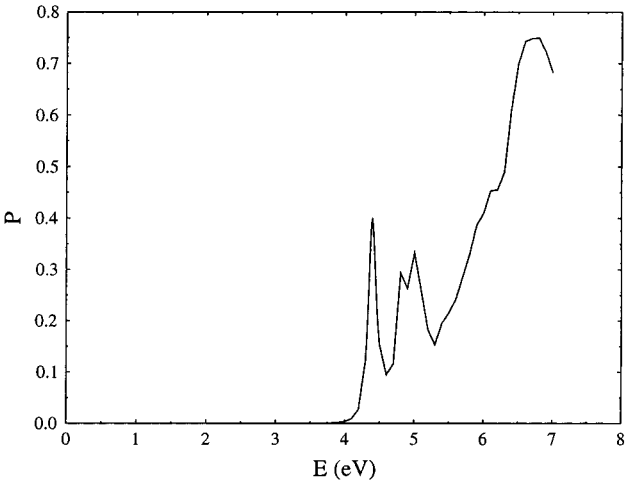

FIGURE 6. Transmission probability vs electron energy for electron tunneling through a water layer ("standard" configuration using model B2, with bare barrier 5 eV).

The possible effect of bound electron states in water on electron transmission probability through water was raised by several workers in the past.[30] In particular, Halbritter[31] has suggested that dipole resonances in the water layers contribute to the transmission; however, our simulations do not support this model. Instead, Peskin et al.[29] have recently identified the source of the resonances seen in our simulations as transient vacancies in the water structure. It should be kept in mind that the existence of other, more rare, structures that support resonances cannot be ruled out by our finite size and finite time simulations.

The effective barrier to electron tunneling in water has been subject to many discussions in the STM literature.[27,28,32] While the absolute numbers obtained vary considerably depending on the systems studied and on experimental setups and conditions, three observations can be made: (a) Tunneling is observed at large tip−surface distances, sometimes exceeding 20 Å.[28,32] (b) The barrier, estimated using a one-dimensional model from the distance dependence of the observed current, is unusually low, of the order of 1 eV in systems involving metals with work functions of 4−5 eV. (c) The numbers obtained scatter strongly: the estimated barrier height may be stated to be 1 ± 1 eV. (d) The apparent barrier height appears to depend on the polarity of the bias potential.

It should be kept in mind that, even in a vacuum STM, the barrier to tunneling is expected to be lower than the work functions of the metals involved due to image effects associated with the fast electronic response of the electrodes.[33] Nevertheless, the reduction in barrier height in the aqueous phase seems to be considerably larger. Taking the vacuum barrier as input in our discussion, let us consider the possible effects of the solvent. These can arise from the following factors: (1) The position, on the energy scale, of the "conduction band" of the pure solvent. By "conduction band", we mean extended electronic states of an *excess* electron in the neutral solvent configuration. (2) The effect of the solvent on the electrode work

function. (3) The hard cores of the atomic constituents—in the present case, the water oxygens—which make a substantial part of the physical space between the electrodes inaccessible to the electron. (4) The possibility that the tunneling is assisted by resonance states supported by the solvent. Such resonances can be associated with available molecular orbitals—this does not appear to be the case in water—or with particular transient structures in the solvent configurations as discussed above.

Factors 2−4 are usually disregarded in theories of electron transfer, while a common practice is to account for the first factor by setting the potential barrier height at a value, below the vacuum level, determined by the contribution of the solvent electronic polarizability. This value can be estimated as the Born energy of a point charge in a cavity of intermolecular dimensions, e.g., a radius of ∼5 au, in a continuum with the proper dielectric constant, here the optical dielectric constant of water, $\epsilon_\infty = 1.88$. This yields $e^2(2a)^{-1}[\epsilon_\infty^{-1} - 1] \approx -1.3$ eV, of the same order as the result of a more rigorous calculation by Schmickler and Henderson,[34] and in agreement with experimental results on photoemission into water.[26b,c] It should be noted that this number was obtained for an infinite bulk of water and should be regarded as an upper limit for the present problem.

Our simulations shed some light on the roles played by the other factors listed above. First, we find that lowering the metal work function by the orientational ordering of water dipoles at the metal surface does affect the tunneling probability (see Figure 4). Second, the occupation of much of the physical space between the electrodes by the impenetrable oxygen cores strongly reduces the tunneling probability. In fact, if these two factors exist alone, i.e., if the electronic polarizability of water is disregarded in the electron−water pseudopotential, the computed tunneling probability is found to be lowered by 1−2 orders of magnitudes relative to that of the vacuum process (see Figure 7 of ref 11). Even including the effect of the water electronic polarizability (i.e., attractive r^{-4} terms) in the two-body electron−water pseudopotential (model A) is not sufficient to reverse this trend, as can be seen in Figure 3. Only by taking into account the full many-body nature of this interaction did we obtain the correct qualitative effect of water, i.e., barrier lowering relative to vacuum.

The estimate of the magnitude of this effect in our simulations can be done in two ways. One is to fit the absolute magnitude of the computed transmission probability to the result obtained from a one-dimensional rectangular barrier of width given by the distance s between the electrodes.[13] This is done in Figure 7 for systems with 1−4 monolayers of water (s = 3.6, 6.6, 10.0, 13.3 Å). It should be emphasized that these results were not statistically averaged over many water configurations, so the absolute numbers obtained should be taken only as examples of a general qualitative behavior. The following points should be noted:

(a) The effective barrier to tunneling computed with the fully polarizable model B2 is reduced by at least 0.5 eV (from the bare value of 5 eV used in these simulations) once a "bulk" has been developed in the water layer, i.e., once the number of monolayers is larger than 2. (Judging from the better-averaged results of Figure 3, the actual barrier lowering is bigger.)

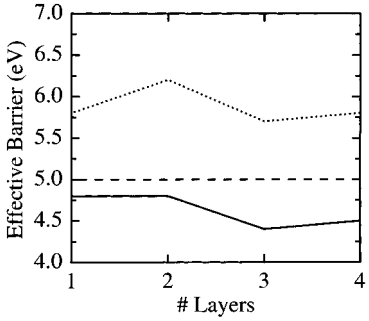

FIGURE 7. Effective one-dimensional barrier height for electron transmission through water, displayed as a function of number of water layers. Solid, dotted, and dashed lines correspond to models B2 and A2 and to the bare (5 eV) barrier, respectively. See text for further details.

(b) The equivalent calculation done with model A1, in which water polarizability is accounted for only on the two-body level, yields an effective barrier higher than the vacuum barrier.

(c) For the very thin layers studied, the effective barrier height depends on the layer thickness. This behavior (which supports a recent experimental observation by Nagy[35]) is expected to saturate once a well-defined bulk is developed.

Another way to discuss the effective simulated barrier is, following common practice in STM studies, to deduce it from the distance dependence of the tunneling probability according to the rectangular barrier relation

$$E_B = \frac{\hbar^2}{8m}\left(\frac{\mathrm{d}\ln I}{\mathrm{d}s}\right)^2 \cong \left[0.95\left(\frac{\mathrm{d}\ln I}{\mathrm{d}s[\text{Å}]}\right)^2\right] \text{eV} \qquad (6)$$

where m is the electron mass, I is the measured current, and s is the tip−sample distance. Note that this formula is only an approximation that becomes less accurate for low barriers. We also disregard possible uncertainties in the determination of s and assume that it is identical to the simulated layer width. Figure 8 shows our results for the transmission probability as a function of barrier thickness, expressed in terms of number of water monolayers (see above for actual distances).[13] The marked differences between results obtained at different incident energies are associated with the observed existence, in the configuration studied, of a barrier resonance at energy ∼4.3 eV (0.7 eV below the vacuum barrier), provided the layer contains at least three water monolayers. This resonance affects the behavior also at considerably lower energies. For example, from the average slope of the line that correspond to model B2 in the upper right panel of Figure 8 (E = 3.6 eV, corresponding to a bare barrier of 1.4 eV), we get, using eq 6, an effective barrier height of ∼0.4 eV, i.e., a reduction of 1 eV. This estimate exceeds the one based on the absolute current. When we go to higher incident energies, the exponential fit that leads to

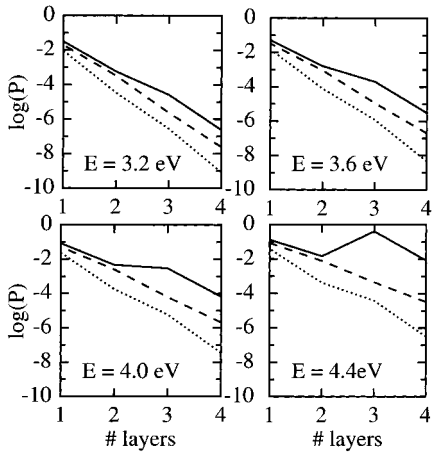

FIGURE 8. Electron transmission probability as a function of the number of water layers at different incident energies. Solid, dotted, and dashed lines correspond to models B2 and A2 and to the bare rectangular barrier (5 eV), respectively.

eq 6 breaks down, and trying to apply it results in vanishingly small barriers. Since this behavior is associated with a barrier resonance, whose existence and energy depend on local structures that evolve in time, we may conclude that the characteristic scatter of data that appears in these measurements[27,28,32] may arise not only because of experimental difficulties but also from intrinsic system properties.

We conclude this discussion with two more comments. First, in the above analysis, we have disregarded the possibility of transient "contamination" of the tunneling medium by foreign ions. Such ions exist in most systems used in underwater STM studies. We have observed in preliminary calculations that placing such an ion in the space of 10−20 Å between the electrodes can have a profound behavior on the tunneling current. This may add another source of scatter in the experimental results. Second, as already discussed, changes in the water structure between the electrodes may appear also as bias-dependent systematic effects, thus the asymmetry in the bias dependence of the barrier height observed in refs 27 and 28 that may be related to the asymmetric transmission properties of orientationally ordered layers.[14]

4. Transmission via Electron Bands

Electron transmission through molecular films depends on the film's electronic structure. For ordered molecular layers, the electronic states may be extended, at least on the scale of the film thickness. In fact, they constitute the precursor of what would become bands in the macroscopic bulk solid. Band structure effects have been, indeed, seen in the LEET experiments of Sanche and co-workers[36] and in the photoemission experiments of Naaman and co-workers.[37] On the theoretical side, we have shown[15,16] that transmission through ordered layers of Ar does show features associated with precursors to band features, even for very thin layers. These features evolve with layer thickness toward their final bulk values and are very sensitive to induced disorder in the layer. Similar ordering effects have been recently observed in simulations of electron transmission through self-assembled alkanethiol monolayers on gold.[38]

5. Conclusions and Perspectives

Traditional electron-transfer phenomena, as well as the growing research and development efforts associated with molecular conductors, require understanding, computing, and predicting electron transmission properties of molecules and molecular layers. In this Account, we have outlined the theoretical methods used to analyze such processes and have investigated some of the electronic and structural factors which affect them, focusing on water as our main example. While neglecting nuclear dynamics in our models was rationalized by time scale arguments, there are obviously situations where such effects cannot be disregarded. Another important effect that was left out of the present discussion is many-electron interactions, most importantly layer charging (e.g., "Coulomb blockades"). These are the next challenges for the computational approach to electron transmission.

This research was supported by the Israel Ministry of Science and by the U.S.-Israel Binational Science Foundation. We thank our collaborators: Professors D. Evans, R. Naaman, U. Peskin, M. Ratner, and T. Seidman, Drs. P. Graf, A. Mosyak, and H. Tal-Ezer, Mr. M. Galperin, and Ms. D. Segal. A.N. thank Professor K. S. Kim for his generous hospitality at Pohang University, South Korea, and Professors K. S. Kim and H. Kang and Mr. J. Soeb for helpful discussions.

References

(1) Kuznetsov, A. M. *Charge Transfer in Physics, Chemistry and Biology*; Gordon and Breach: New York, 1995.

(2) For earlier work on electron transmission, see: Marsolais, R. M.; Carter, E. A.; Pfluger, P. Excess electrons in dielectric media. In *Hot electron transport in condensed organic dielectrics*; Jay-Gerin, J.-P., Ferradini, C., Eds.; CRC Press: Boca Raton, FL, 1991; Chapter 2. For a review of LEET results, see: Sanche, L. Primary interactions of low energy electrons in condensed matter. In *Hot electron transport in condensed organic dielectrics*; Jay-Gerin, J.-P., Ferradini, C., Eds.; CRC Press: Boca Raton, FL, 1991.

(3) Landauer, R. One-Dimensional Lattices. *Philos. Mag.* **1970**, *21*, 863.

(4) Miller, W. H.; Schwartz, S. D.; Tromp, J. W. Quantum Mechanical Rate Constants for Bimolecular Reactions. *J. Chem. Phys.* **1983**, *79*, 4889.

(5) Liang, C.; Newton, M. D. Ab Initio Studies of Electron-Transfer. *J. Phys. Chem.* **1992**, *96*, 2855; **1993**, *97*, 3199 and references therein. Joachim, C.; Gimzewski, J. K.; Schlitter, R. R.; Chavy, C. Electronic Transparence of a Single c_{60} Molecule. *Phys. Rev. Lett.* **1995**, *74*, 2102 and references therein. Kemp, M.; Roitberg, A.; Mujica, V.; Wanta, T.; Ratner, M. A. Molecular Wires-Extended Coupling and Disorder Effects. *J. Phys. Chem.* **1996**, *100*, 8349 and references therein.

(6) Barnett, R. N.; Landmann, U.; Cleveland, C. L. Electron Localization in Water Clusters. 1. Electron−Water Pseudopotential. *J. Chem. Phys.* **1988**, *88*, 4420.

(7) Tal-Ezer, H.; Kosslof, R. An Accurate and Efficient Scheme for Propagating the Time Dependent Schrodinger Equation. *J. Chem. Phys.* **1984**, *81*, 3967. Kosloff, R. Time-Dependent Quantum-Mechanical Methods for Molecular Dynamics. *J. Phys. Chem.* **1988**, *92*, 2087.
(8) Seidman, T.; Miller, W. H. Quantum Mechanical Reaction Probabilities via a Discrete Variable Representation-Absorbing Boundary Condition Greens Function. *J. Chem. Phys.* **1992**, *97*, 2499.
(9) Saad, Y. *Iterative methods for sparse linear systems*; PWS Publishing Co.: Boston, MA, 1996.
(10) Barnett, R. N.; Landman, U.; Nitzan, A. Primary Events Following Electron Injection into Water and Adsorbed Water Layers. *J. Chem. Phys.* **1990**, *93*, 6535−6542.
(11) Mosyak, A.; Nitzan, A.; Kosloff, R. Numerical Simulations of Electron-Tunneling Water. *J. Chem. Phys.* **1996**, *104*, 1549−1560.
(12) Mosyak, A.; Graf, P.; Benjamin, I.; Nitzan, A. Electron Tunneling through Water Layers: Effect of Polarizability. *J. Phys. Chem. A* **1997**, *101*, 429−433.
(13) Benjamin, I.; Evans, D.; Nitzan, A. Electron Tunneling through Water Layers: Effect of Layer Structure and Thickness. *J. Phys. Chem.* **1997**, *106*, 6647−1954.
(14) Benjamin, I.; Evans, D.; Nitzan, A. Asymmetric Tunneling through Ordered Molecular Layers. *J. Chem. Phys.* **1997**, *106*, 1291−1293.
(15) Naaman, R.; Haran, R.; Nitzan, A.; Evans, D.; Galperin, M. Electron Transmission through Molecular Layers. *J. Phys. Chem. B* **1998**, *102*, 3658−3668.
(16) Haran, A.; Kadyshevitch, A.; Cohen, H.; Naaman, R.; Evans, D.; Seidman, T.; Nitzan, A. Electron Transmission through Band-Structure in Organized Organic Thin-Films. *Chem. Phys. Lett.* **1997**, *268*, 475.
(17) Jo, S. K.; White, J. M. Low-Energy (less-than-1 ev) Electron Transmission through Condensed Layers of Water. *J. Chem. Phys.* **1991**, *94*, 5761.
(18) Rostkier, D.; Urbakh, M.; Nitzan, A. Electron Tunneling through a Dielectric Barrier. *J. Chem. Phys.* **1994**, *101*, 8224.
(19) Buttiker, M.; Landauer, R. Tranersal Time for Tunneling. *Phys. Scr.* **1985**, *32*, 429.
(20) Barnett, R. N.; Landman, U.; Nitzan, A. Relaxation Dynamics Following Transition of Soluated Electrons. *J. Chem. Phys.* **1989**, *90*, 4413; Dynamics of Excess Electron Migration, Soluation and Spectra in Polar Molecular Clusters. *J. Chem. Phys.* **1989**, *91*, 5567.
(21) Dang, L. X. The Nonadditive Intermolecular Potential for Water Revised. *J. Chem. Phys.* **1992**, *97*, 2659. Benjamin, I. Electronic Spectra in Bulk Water and at the Water Liquid/Vapor Interface. Effect of Solvent and Solute Polarizabilities. *Chem. Phys. Lett.* **1998**, *287*, 480.
(22) Staib, A.; Borgis, D. Molecular-Dynamics Simulation of an Excess Charge in Water Using Mobile Gaussian-Orbitals. *J. Chem. Phys.* **1995**, *103*, 2642.
(23) Hautman, J.; Halley, J. W.; Rhee, Y.-J. Molecular Dynamics Simulation of Water between Two Ideal Classical Metal Walls. *J. Chem. Phys.* **1989**, *91*, 467.
(24) Spohr, E. Computer Simulation of the Water/Platinum Interface. *J. Phys. Chem.* **1989**, *93*, 6171.
(25) Benjamin, I.; Nitzan, A. Unpublished results.
(26) See, e.g.: (a) Theil, P. A.; Madey, T. E. The interaction of water with solid surfaces fundamental aspects. *Surf. Sci. Rep.* **1987**, *7*, 211. (b) Gurevich, Yu. Y.; Pleksov, Yu. Y.; Rotenberg, Z. A. *Photoelectrochemistry*; Consultant Bureau: New York, 1980. (c) Furtak, T. E.; Kliewer, K. L. Photoemission into Electrolytes: A New Tool in Solid State and Interfacial Physics. *Comments Solid State Phys.* **1982**, *10*, 103.
(27) Pan, J.; Jing, T. W.; Lindsay, S. M. Tunneling barriers in electrochemical STM. *J. Chem. Phys.* **1994**, *98*, 4205.
(28) Hong, Y. A.; Hahn, J. R.; Kang, H. Electron-Transfer through Interfacial Water Layer Studied by STM. *J. Chem. Phys.* **1998**, *108*, 4367. Hahn, J. R.; Hong, Y. A.; Kang, H. Electron Tunneling across an Interfacial Water Layer inside an STM Junction: Tunneling Distance, Barrier Height and Water Polarization Effect. *Appl. Phys. A* **1998**, *66*, S467.
(29) Peskin, U.; Edlund, A.; Baron, I.; Galperin, M.; Nitzan, A. To be published.
(30) Saas, J. K.; Gimzewski, J. K. Solvent Dynamical Effects in Scanning Tunneling Microscopy with a Polar Liquid in the Gap. *J. Electroanal. Chem.* **1991**, *308*, 333.
(31) Halbritter, J.; Repphun, G.; Vinzelberg, S.; Staikov, G.; Lorentz, W. J. Tunneling Mechanisms in Electrochemical STM-Distance and Voltage Tunneling Spectroscopy. *Electrochim. Acta* **1995**, *40*, 1385.
(32) Christoph, R.; Siegenthaler, H.; Rohrer, H.; Wiese, W. In Situ Scanning Tunneling Microscopy at potential Controlled Ag(100) Substrates. *Electrochim. Acta* **1989**, *34*, 1011.
(33) Lang, N. D. Apparent Barrier Height in Scanning Microscopy. *Phys. Rev.* **1988**, *B37*, 10395.
(34) Schmickler, W.; Henderson, D. J. A Model for the Scanning Tunneling Microscope Operating in an Electrolyte Solution. *J. Electroanal. Chem.* **1990**, *290*, 283.
(35) Nagy, G. Water Structure at the Graphite(0001) Surface by STM Measurements. *J. Electroanal. Chem.* **1996**, *409*, 19−23.
(36) Caron, L. G.; Perluzzo, G.; Bader, G.; Sanche, L. Electron Transmission in the Energy Gap of Thin Films of Argon, Nitrogen, and *n*-Hexane. *Phys. Rev. B* **1986**, *33*, 3027.
(37) References 15 and 16 and references therein.
(38) Wampler, R.; Evans, D. Electron Transmission through Self-Assembled Monolayers. To be published.

AR970267B